Hindawi
Advances in Civil Engineering
Volume 2021, Article ID 3208974, 11 pages
https://doi.org/10.1155/2021/3208974

*Research Article*

# Deformation Failure and Support Test of Surrounding Rock in Deep Arched Roadway with Straight Wall

**Shuqi Pan,[1,2] Shuaitao Liu,[1,2] Liming Cao,[3] Jianqiang Guo,[3] and Chao Yuan [3]**

[1]*State Key Laboratory of Coking Coal Exploitation and Comprehensive Utilization, China Pingmei Shenma Group, Pingdingshan 467099, Henan, China*
[2]*China Pingmei Shenma Energy and Chemical Group Corporation Limited, Pingdingshan 467000, Henan, China*
[3]*School of Resources, Environment and Safety Engineering, Hunan University of Science and Technology, Xiangtan 411201, Hunan, China*

Correspondence should be addressed to Chao Yuan; yuanchaozh1@126.com

Received 13 July 2021; Accepted 19 August 2021; Published 31 August 2021

Academic Editor: Jie Liu



The deformation and failure of the uphill roadway on the 3rd horizontal track in the No. 6 Mine of Pingdingshan Coal Group was taken as the engineering background. The similar simulation material of the roadway surrounding rock with quartz sand as the aggregate, cement as the cementing agent, and gypsum powder as the regulator was selected. Through mechanical tests on 25 sets of specimens with different proportions, the best proportion of similar simulated materials for simulating the deformation and failure of the surrounding rock of the roadway was obtained. Later, a large-scale deep mine roadway simulation test system independently developed by the company was used to carry out the roadway deformation and failure test. First, load the test body to the set initial stress state, and then carry out the full-face excavation and unloading of the roadway; finally, load it in the vertical direction until the roadway wall is damaged. It can realize the actual effect of simulation of roadway deformation and failure under the path of "high stress + internal unloading + stress adjustment." The results showed that after the deep roadway is excavated with preload and high stress, the surrounding rock deformation, failure, and instability of the roadway mainly experience 3 periods: the first period is the period of uniform deformation of the roadway surrounding rock, the second period is the development period of the roadway surrounding rock slab structure, and the third period is the period of instability of the roadway surrounding rock slab structure. Combined with the time period of deformation and failure of the surrounding rock of the roadway, the damage scope of the surrounding rock and the actual situation of the site engineering. A step-by-step combined roadway repair and support plan of "bolt mesh + shotcrete + full-face hollow grouting anchor cable" with hollow grouting anchor cable as the core was determined. The stability of the repaired roadway has been significantly improved, ensuring the long-term use of the roadway.

## 1. Introduction

Energy and mineral resources are important factors restricting the development of the national economy of all countries in the world. With the reduction and depletion of shallow resources in various countries, the mining depth of coal and other mineral resources in countries around the world is increasing year by year, and the scale is getting bigger and bigger. Various types of wellbore, roadway, and cavern need to be excavated before mining. The smooth flow and stability of the roadway engineering is the basic prerequisite to ensure the normal production of coal mines. At the same time, roadway maintenance and disaster prevention have become a key issue of mine economic efficiency and production safety and even determine the feasibility of resource development and the issue of sustainable development [1–3].

The unexcavated rock mass of the underground mine roadway is in a three-dimensional stress state. After excavation and unloading, the surrounding rock of the roadway close to the goaf is in a two-dimensional stress state, and the rock mass after excavation and unloading will be subjected to stress adjustment and other effects, which in turn induces geological disasters such as large deformation, roof fall, and

spalling rib in the surrounding rock of the roadway, which seriously hinders the safe and efficient production of the mine. Therefore, the entire force process of the surrounding rock of the roadway can be described as "high ground stress + excavation unloading + stress adjustment." The key problem of studying the deformation and failure mode of the surrounding rock of the roadway and determining the support parameters of the roadway is the problem of the deformation and failure of the surrounding rock of the roadway during the deep mining process. Many rock mechanics workers have carried out systematic research through various methods and means such as theoretical analysis, similar simulation, numerical calculation, and field measurement [4–6]. Tang and Liang's method of similar material simulation is used to analyze the mining problems of irregular coal roadways, the usability of the upward mining method is studied, and the surrounding rock failure mechanism is explored [7]. Xu et al. based on the related theories of geological models obtained similar materials suitable for tunnel lining through matching experiments. Physical parameters such as uniaxial compressive strength and cohesion of similar materials are studied, which provides theoretical guidance for tunnel lining [8]. Zhou et al. used a roadway physical similar material model with circular and different-sized straight-wall arched holes to study the influence of the roadway section curvature radius on the failure [9]. Liu et al. conducted a rockburst simulation test on a cubic granite sample with cylindrical through-holes, analyzed the fracture shape and energy changes of rockburst under different lateral stresses, and discussed the acoustic emission sequence during the rockburst process, time-frequency, and space-time evolution characteristics [10]. Jing et al. relied on the self-developed deep underground engineering structure instability full process simulation test system, conducted large-scale physical model tests on the deformation and fracture evolution characteristics of the surrounding rock of the roadway, and revealed the internal stress and deformation and fracture evolution of the surrounding rock law [11]. In addition, in the control of surrounding rock of the roadway, Li et al. combined the finite element method and elastoplastic mechanics to derive the butterfly-shaped plastic zone of the surrounding rock of the roadway and revealed the mechanism of the nonuniform deformation of the deep rock mass [12]. Kang et al. proposed the coordinated control concept of high-pressure anchor note and shotcreting for the surrounding rock of a weak and broken roadway in a thousand-meter deep well. The performance of grouting bolts, anchor cables, and grouting materials and the effect of grouting are studied. A coordinated control technology of high prestress anchor rods, anchor cable support-high-pressure split grouting modification-surface shotcreting has been formed [13]. Xie et al. proposed the supporting technology of anchoring and jetting strengthened pressure-bearing arch, which integrates dense and high-strength anchor pressure-bearing arch, thick-layer steel mesh and shotcrete arch, and lagging grouting-reinforced arch, and clarified the mechanism of arching and strengthening support [14]. Yang et al. used theoretical analysis to obtain the deformation mechanism of the surrounding rock of a large-section thick-top coal roadway. And a large amount of data has been obtained through a combination of field practice and numerical simulation, and combined with the obtained data, a combined support technology of "high prestressed anchor cable + U-shaped anchor cable composite truss" is proposed [15]. Yu et al. explored the method of controlling the roof deformation of the inclined coal seam, numerical simulation and theoretical analysis were used to establish mechanical models of different zones, and different roof support resistance and deformation conditions were obtained. And according to the deformation characteristics of the roof load, the function of the entire support system is analyzed [16]. Xiong et al. explored the asymmetric deformation and failure characteristics of the surrounding rock of a right-angle trapezoidal roadway, and numerical simulation methods are used to conduct in-depth research on the horizontal and vertical damage of surrounding rock, and it is found that the symmetrical part along the dip of the coal seam shows obvious uneven stress distribution [17]. Liu et al. conducted multiple sets of indentation experiments on four types of rocks with different materials by using the constant section method. The main purpose of the experiment was to study the overall crushing of rocks under different indentations [18, 19].

At present, in terms of deep roadway stability and control technology, although some large-scale test systems have emerged, due to the limitations of loading capacity, simulation method, and measurement technology, they cannot fully meet the requirements of true reproduction of the deep roadway excavation and stress adjustment process. As a result, the research on some key theoretical issues, such as the failure mechanism of surrounding rock and the supporting mechanism under complex conditions, is still greatly restricted [20, 21]. In order to study the internal excavation unloading of the surrounding rock of a deep arched roadway, and the deformation and failure process and mechanism of surrounding rock induced by stress adjustment in the later stage, the self-developed large-scale deep mine roadway simulation test system was used to carry out a similar simulation test of "high ground stress + excavation unloading + stress adjustment." The ways of deformation and failure instability of the surrounding rock of the roadway were analyzed; on this basis, a step-by-step combined roadway repair and support program of "anchor mesh and shotcrete + full-face hollow grouting anchor cable" with the hollow grouting anchor cable as the core was determined, and engineering verification was carried out, and the surrounding rock control of the roadway was in good condition.

## 2. General Situation and Deformation Characteristics of Roadway Engineering

*2.1. Overview of Roadway Engineering.* The cross section of the uphill roadway on the third horizontal track of Pingmei's No. 6 Mine is a straight-wall arch; the width is 4.4 m and the height is 3.5 m. The supporting scheme adopts the combined

support of bolt, mesh, cable, and shotcrete. The side and roof bolts adopt $\Phi 20\,\text{mm} \times L2000\,\text{mm}$ ordinary threaded steel bolts, and the spacing between rows is $700\,\text{mm} \times 700\,\text{mm}$. The anchor adopts $\Phi 17.8\,\text{mm} \times L6000\,\text{mm}$ steel strand, and the spacing between rows is $1500\,\text{mm} \times 1400\,\text{mm}$; the steel mesh is $\Phi 3.5\,\text{m} \times 50\,\text{mm}$; the cement used for shotcreting is No. 32.5 ordinary Portland cement, and the volume ratio of cement to sand is 1 : 2.5; the thickness is 100 mm, as shown in Figure 1.

### 2.2. Deformation Characteristics and Mechanical Mechanism of Surrounding Rock in Roadway

*2.2.1. Deformation Characteristics of Roadway Surrounding Rock.* Through field investigation, the deformation and failure of the roadway has the following characteristics: the two ribs of the roadway are severely squeezed inward, spalling rib is serious, and the maximum deformation between the two sides is as high as 1900 mm. The bolt of the gang part fell off, and the roadway section is Σ-shaped. The roof of the roadway has a large amount of sinking, a large number of net pockets appear locally, and the top anchor cable appears to be trapped in the surrounding rock and broken, and the maximum deformation of the roof and floor reaches 1200 mm. The deformation and failure form of the roadway is shown in Figure 2.

*2.2.2. Deformation Mechanics Mechanism of Surrounding Rock of Roadway.* In a high-stress environment, there is a large deformation in the deep roadway, and the control of the surrounding rock is more difficult. (1) After excavation, the stability of the surrounding rock of the roadway becomes worse, and a large number of joints and cracks are generated in the surrounding rock. And as time goes by, small cracks develop and expand, and the plastic zone quickly shifts to the deep part. If the surrounding rock of the roadway is not effectively controlled, when the damage and deformation of the surrounding rock develops to a certain extent, spalling rib and roof fall will occur. (2) Under the action of high ground stress, the surrounding rock of the roadway will continue to deform with the increase of time; that is, the rheological properties of the surrounding rock are obvious. The supporting structure is constantly subjected to high loads brought by the surrounding rock, which eventually causes the roadway supporting structure to exceed the allowable bearing strength and fail. At the same time, the surrounding rock has accelerated its deformation, the plastic zone area has increased sharply, and the roadway has severe slack and roof subsidence.

## 3. Large-Scale Similar Simulation Test of Deep Roadway

### 3.1. Overview of Roadway Engineering

*3.1.1. Selection of Similar Materials.* Based on the development principles and similar conditions of similar materials, we have an in-depth understanding of the characteristics of various similar materials in the current engineering geomechanics model. For similar raw materials, quartz sand is selected as aggregate, cement is used as cementing agent, and gypsum powder is used as regulator. Due to the adjustment of the ratio of the composition of similar raw materials, the main mechanical parameters of the composite material will be greatly changed. Therefore, 25 groups of different ratios were designed using the orthogonal method (see Table 1). The composite material has the advantages of simple processing technology, low material cost, reasonable aggregate gradation, fast drying, nontoxic and harmless, and the like. Figure 3 shows similar raw materials.

*3.1.2. Mechanical Strength Test of Similar Materials.* The main physical and mechanical parameters such as compressive strength, Poisson's ratio, elastic modulus, internal friction angle, cohesion, and tensile strength can be tested by the equipment RMT-150 rock mechanics test system. Through the abovementioned standard specimen mechanics test, the bulk density, compressive strength, tensile strength, elastic modulus, internal friction angle, cohesion, and other main physical and mechanical parameters of 25 groups of different material ratio specimens were measured (see Table 1). The damaged state of the specimen is shown in Figure 4.

Through the analysis of the main physical and mechanical parameters of 225 specimens, it is found that the physical and mechanical strength parameters of similar materials with quartz sand as the aggregate have a wide range of changes. For example, the bulk density of similar materials is in the range of 18.1~19.9 $\text{kN/m}^3$, the compressive strength is in the range of 0.53~13.71 MPa, the cohesion is in the range of 0.08~0.17 kPa, the internal friction angle is in the range of 28.4°~33.8°, and the elastic modulus is in the range of 0.53~0.86 GPa. Therefore, the similar materials we have selected can simulate most of the deformation and failure of deep roadways.

*3.1.3. Selection of the Ratio of Similar Materials.* The uphill roadway of the third horizontal track in No. 6 Mine of Pingmei Coal Co., Ltd. is a rock roadway with argillaceous siltstone lithology, through the experimental determination of the physical and mechanical parameters of argillaceous siltstone. Table 2 shows the measurement results of the main mechanical parameters of the surrounding rock under actual working conditions. The select optimal similarity ratio between mechanical parameters of similar materials and mechanical parameters of surrounding rock under actual working conditions is as follows [22]: the bulk density similarity ratio is 1 : 1, the strength similarity ratio is 1 : 6, the stress similarity ratio is 1 : 6, the force similarity ratio is 1 : 216, and the internal friction angle similarity ratio is 1 : 1.

Based on the main mechanical parameters of the surrounding rock under actual working conditions, and combined with the main mechanical parameters obtained

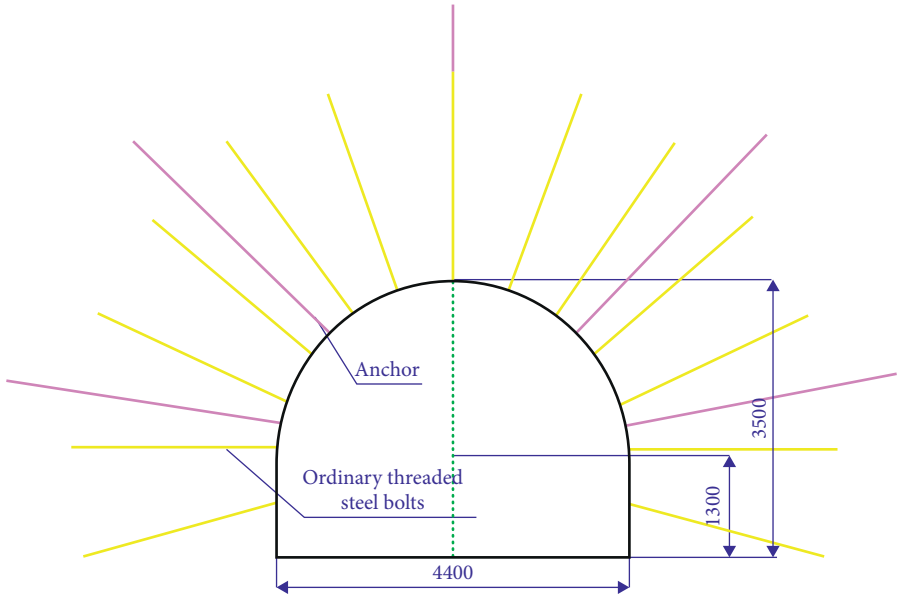


Figure 1: Original support plan.

Figure 2: Spalling rib forms of surrounding rocks in deep roadways.

from the abovementioned different ratio material test specimens, the comparative analysis is carried out; it is most reasonable to select similar materials with quartz sand as aggregate with a ratio of 1 : 0.13 : 0.2 as the simulation test of argillaceous siltstone.

*3.2. Similar Model Test System Composition.* In order to effectively simulate the deformation and failure characteristics of deep roadway surrounding rock under high ground stress environment, we have developed a large-scale deep mine roadway simulation test system (Figure 5), and the model is 1500 mm long, 1000 mm wide, and 1500 mm high. The test system is mainly composed of a model reaction bench device, a high-pressure water injection system, a hydraulic loading system and a data collection device. The up and down, left and right, front and rear pressurization and safety and stability of the model are completed by intelligent hydraulic devices. Data collection is mainly completed by the cooperation of intelligent hydraulic control device, grating micro multipoint displacement acquisition and analysis system and stress and strain data collection software (DHDAS2013).

*3.3. Model Making and Roadway Excavation Loading Test*

*3.3.1. Model Making.* The size of the model is 1 500 mm × 1 000 mm × 1 500 mm, the internal filling of the model is completed by layered paving and air-drying, and the specific operation steps are as follows: perform layer-by-layer weighing according to the ratio of similar materials determined above ⟶ stir evenly weighed similar materials with a mixer ⟶ pave and compact materials in layers from bottom to top in the internal space of the model ⟶ buried test components around the simulated roadway elevation and the cross section at a distance of 200 mm from the model opening, and contains pressure cell and strain brick.

*3.3.2. Excavation and Loading of Model Roadway.* The excavation model of the roadway is a straight-wall arch, the radius of the round arch is 150 mm, and the height of the straight wall is 150 mm. Load a pressure of 1.0 MPa on the top, bottom, left and right, and front and back of the model. When the load is loaded to the predetermined value, keep the load size unchanged, and simulate the excavation of the roadway according to the full-section method. And the excavation is carried out circularly along the axis of the roadway, each excavation length is 50 mm, and a total of 20 excavations are completed. Pause the excavation after each excavation step and record the stable data. After the excavation of the roadway is completed, the original surrounding rock stress state is maintained for 4 hours. After 4 hours, keep the other pressures of the model unchanged, and gradually load the pressure in the vertical direction until the roadway surrounding rock spalling rib. The vertical stress at which the surrounding rock of the roadway failed was

Table 1: Main physical and mechanical parameters of different proportioning specimens.

| Serial number | Material ratio Quartz sand: cement: plaster | Volumetric weight (kN/m$^3$) | Tensile strength (MPa) | Compressive strength (MPa) | Elastic modulus (GPa) | Internal friction angle (°) | Cohesion (kPa) |
|---|---|---|---|---|---|---|---|
| 1 | 1 : 0.30 : 0.70 | 19.1 | 0.46 | 5.33 | 0.65 | 32.4 | 0.15 |
| 2 | 1 : 0.40 : 0.60 | 18.5 | 0.56 | 6.34 | 0.63 | 31.5 | 0.13 |
| 3 | 1 : 0.50 : 0.50 | 19.0 | 0.83 | 7.57 | 0.54 | 30.6 | 0.14 |
| 4 | 1 : 0.60 : 0.40 | 18.9 | 1.01 | 8.02 | 0.77 | 29.8 | 0.16 |
| 5 | 1 : 0.70 : 0.30 | 19.1 | 1.51 | 13.01 | 0.78 | 29.6 | 0.11 |
| 6 | 1 : 0.15 : 0.34 | 18.9 | 0.23 | 2.27 | 0.81 | 28.3 | 0.12 |
| 7 | 1 : 0.19 : 0.30 | 19.9 | 0.26 | 3.80 | 0.86 | 28.6 | 0.14 |
| 8 | 1 : 0.25 : 0.24 | 19.3 | 0.62 | 6.07 | 0.83 | 28.4 | 0.13 |
| 9 | 1 : 0.30 : 0.19 | 19.0 | 0.64 | 7.11 | 0.84 | 32.6 | 0.17 |
| 10 | 1 : 0.34 : 0.15 | 19.2 | 0.89 | 8.99 | 0.79 | 32.8 | 0.11 |
| 11 | 1 : 0.11 : 0.23 | 18.6 | 0.06 | 1.64 | 0.77 | 33.6 | 0.10 |
| 12 | 1 : 0.13 : 0.20 | 19.3 | 0.13 | 2.20 | 0.65 | 31.7 | 0.15 |
| 13 | 1 : 0.17 : 0.16 | 18.6 | 0.27 | 3.51 | 0.69 | 31.5 | 0.14 |
| 14 | 1 : 0.20 : 0.13 | 18.8 | 0.34 | 4.27 | 0.62 | 32.0 | 0.09 |
| 15 | 1 : 0.24 : 0.19 | 18.6 | 0.41 | 5.12 | 0.66 | 29.6 | 0.08 |
| 16 | 1 : 0.08 : 0.18 | 18.7 | 0.05 | 0.53 | 0.64 | 31.7 | 0.11 |
| 17 | 1 : 0.10 : 0.15 | 18.3 | 0.07 | 1.50 | 0.58 | 33.6 | 0.12 |
| 18 | 1 : 0.56 : 0.56 | 18.4 | 0.11 | 1.79 | 0.59 | 33.5 | 0.14 |
| 19 | 1 : 0.15 : 0.10 | 18.3 | 0.13 | 1.95 | 0.58 | 32.4 | 0.07 |
| 20 | 1 : 0.18 : 0.08 | 18.6 | 0.20 | 1.80 | 0.62 | 32.7 | 0.13 |
| 21 | 1 : 0.06 : 0.14 | 18.2 | 0.04 | 0.71 | 0.63 | 30.1 | 0.11 |
| 22 | 1 : 0.08 : 0.12 | 18.3 | 0.05 | 1.01 | 0.71 | 32.9 | 0.09 |
| 23 | 1 : 0.10 : 0.11 | 18.1 | 0.06 | 1.62 | 0.72 | 33.5 | 0.14 |
| 24 | 1 : 0.12 : 0.08 | 18.7 | 0.17 | 2.20 | 0.54 | 33.8 | 0.13 |
| 25 | 1 : 0.14 : 0.06 | 18.6 | 0.13 | 2.06 | 0.53 | 30.3 | 0.12 |

Note: The quality of water in the process of mixing different materials is always one-sixth of the total mass of the materials.


Figure 3: Similar raw materials.

Figure 4: Specimen deformation and failure.

2.4 MPa. The failure characteristics of the early, initial stages, and late stages of roadway excavation are shown in Figure 6.

*3.3.3. Analysis of Test Results.* From the analysis of the failure characteristics before and after the excavation of the roadway in Figure 6, it is found that the surrounding rock of the roadway is in a uniform deformation stage at the initial stage of the roadway excavation, as shown in Figure 6(b). Later, as the vertical pressure gradually increased, the cracks in the surrounding rock of the roadway ledge formed a thin layer of rock slab; however, the rock slabs are not completely separated, forming a combined rock slab, showing a slab cracked structure. This phenomenon is similar to the failure of surrounding rock slabs in deep roadways, indicating that the simulation test is reasonable and effective. When the vertical pressure increases to 2.4 MPa, the slab cracking structure further develops, and the slab cracking structure suddenly loses stability as a whole, separates from the roadway wall, and ruptures. The extent of cracking damage of the surrounding rock slab at the roadway ledge gradually increases and runs through the axial direction of the entire roadway, and the roadway is damaged and unstable, as shown in Figure 6(c).

Figure 7 shows the surrounding rock deformation after the excavation of the roadway. In the initial stage of unloading of the surrounding rock of the roadway, the deformation rates of the two sides of the roadway and the roof and floor are

Table 2: Main mechanical parameters of surrounding rock under actual working conditions.

| Mechanical parameters | Volumetric weight ($kN/m^3$) | Tensile strength (MPa) | Compressive strength (MPa) | Elastic modulus (GPa) | Internal friction angle (°) | Cohesion (kPa) |
|---|---|---|---|---|---|---|
| | 19.3 | 0.78 | 13.2 | 3.9 | 31.7 | 32.4 |


(a) (b)

Figure 5: Similar model test system. (a) Positive. (b) Side.

(a) (b) (c)

Figure 6: Failure characteristics before and after roadway excavation. (a) Before roadway excavation. (b) Initial stages of roadway excavation. (c) Late stages of roadway excavation.

relatively low, and the amount of deformation is relatively small. The deformation of the two sides is 8.6 mm, and the deformation of the top and bottom plates is 7.0 mm. With the gradual increase of vertical pressure, the deformation rates of the two sides of the roadway and the roof and floor have increased to varying degrees. However, the growth rate of the two sides is greater than that of the roof and floor. The deformation of the two sides after 12 hours of roadway excavation is 60.8 mm, and the deformation of the roof and floor is 33.8 mm. In addition, by comparing and analyzing Figures 2 and 7, it can be found that under actual conditions, the serious fragmentation phenomenon of the two sides of the surrounding rock of the roadway echoes the large displacement of the two sides in the conclusions of similar simulation experiments. Through the comparison of the deformation characteristics, it can be clearly found that the deformation and failure characteristics of the surrounding rock of the roadway under actual working conditions are very similar to the results obtained by the similar simulation experiment, so it can be further determined that the similar simulation experiment is effective.

Through further analysis in Figures 6 and 7, it is found that the deformation and failure of the surrounding rock of the roadway mainly experience 3 periods. The first period is the period of uniform deformation of the surrounding rock of the roadway, and the deformation rate and amount of deformation are relatively small. This period of time is

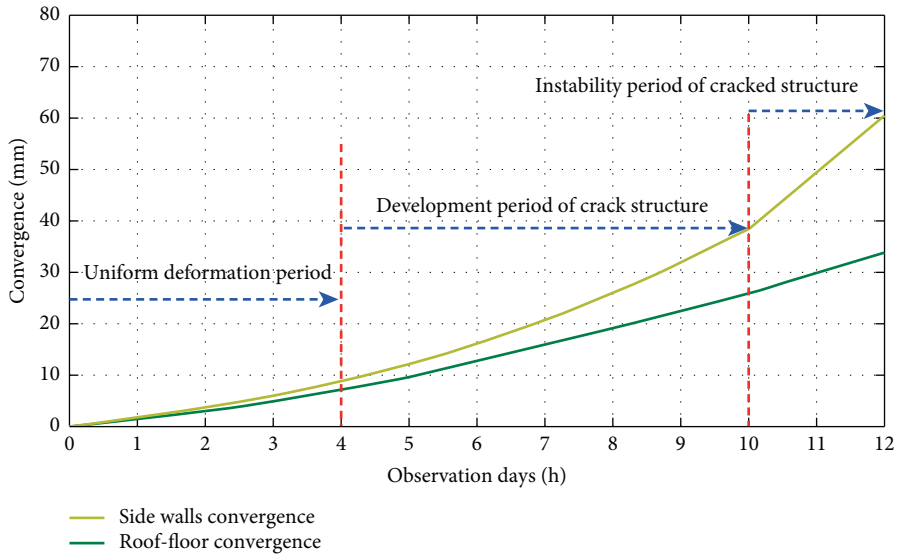


Figure 7: Deformation characteristic curve of roadway surrounding rock.

mainly due to the excavation and unloading of the surrounding rock of the roadway, a large amount of elastic strain energy stored in the surrounding rock mass is released, and a large number of meso cracks are generated in the roadway surrounding rock, and it is distributed more evenly around the roadway, and the surrounding rock shows almost uniformly coordinated deformation as a whole, but the duration of uniformly coordinated deformation is relatively short. The second period is the development period of the slab crack structure of the surrounding rock of the roadway. As the unloading degree of the surrounding rock of the roadway weakens, after that, it is mainly affected by the deviator stress, and the deformation rate and amount of deformation gradually increase. A large number of mesoscopic cracks develop into macroscopic cracks, forming a composite rock slab that is not completely separated, presenting a slab cracked structure, and the rock block bulges toward the empty surface of the roadway. This stage is the main period of large deformation of the surrounding rock of the roadway, and as it continues, it takes a long time. The third period is the instability period of the slab crack structure of the surrounding rock of the roadway. The energy accumulated by the deformation of the surrounding rock exceeds the energy storage limit of the slab cracked structure. The slab cracking structure suddenly loses stability, the slab cracked rock block instantly breaks into blocks and separates from the roadway wall, and the strain energy is suddenly released and converted into rock fragmentation dissipated energy and ejection kinetic energy, thrown into the roadway space, and the damage area is along the radial direction of the roadway, extending to form a V-shaped groove on the roadway wall [23].

## 4. Roadway Support Principle and Support Plan

*4.1. Roadway Support Principle.* The high ground stress environment and roadway excavation unloading are the root causes of large deformation and failure instability of the deep roadway surrounding rock. According to the 3 periods of deformation and failure of the deep roadway surrounding rock in the large-scale similar simulation test, the roadway surrounding rock support is also needed to start from 2 time points: ① The support at the first time point is mainly the initial support during the unloading period of the surrounding rock of the roadway. Active support should be carried out immediately after the excavation of the roadway, timely restrain the occurrence of discontinuous expansion phenomena such as separation, slippage, crack opening, new cracks, etc., of the surrounding rock of the roadway inside and outside the anchorage zone, and prevent the roof falling and spalling rib of the roadway surrounding rock. ② The support at the second time point is mainly to strengthen the support of the surrounding rock of the roadway, design reasonable support structure and support parameters, and carry out high-pressure grouting. The weak and broken surrounding rock is filled and cemented, the loose structure and mechanical properties of the surrounding rock mass are improved, the integrity and continuity of the surrounding rock are enhanced, and the permanent stability of the roadway is realized.

*4.2. Calculation of Failure Range of Surrounding Rock of Roadway.* The damage range of the surrounding rock of the roadway is the key to the design of the roadway support. The formation and expansion of the plastic zone is always accompanied by the deformation and failure of the surrounding rock of the roadway. Therefore, the design of surrounding rock support can be carried out in accordance with the theory of plastic zone. According to the existing research results [24], the mechanical model of the plastic zone of the nonisobaric circular roadway surrounding rock with $r$ and $\theta$ is shown in Figure 8. The implicit equation of the plastic zone boundary of the surrounding rock of the roadway is

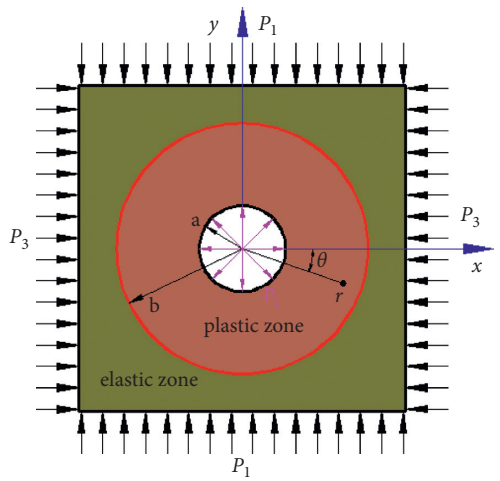


Figure 8: Fore model of rock surrounding circular roadway in an inhomogeneous stress field.

$$
\begin{aligned}
f(r,\theta) = {} & \left[P_1(\lambda-1)\cos 2\theta\left(1-\frac{2a^2}{r^2}+\frac{3a^4}{r^4}\right)-\frac{a^2(\lambda P_1+P_1)}{r^2}+\frac{2a^2P_i}{r^2}\right]^2 \\
& +\left[P_1(\lambda-1)\sin 2\theta\left(1+\frac{2a^2}{r^2}-\frac{3a^4}{r^4}\right)\right]^2 \\
& -\frac{(1-\cos 2\varphi)}{2}\left\{\left[P_1(\lambda+1)-\frac{2P_1(\lambda-1)a^2\cos 2\theta}{r^2}\right]^2-4c^2\right\} \\
& -2c\sin 2\varphi\left[P_1(\lambda+1)-\frac{2P_1(\lambda-1)a^2\cos 2\theta}{r^2}\right]-4c^2.
\end{aligned}
\tag{1}
$$

For noncircular roadways, the calculation of plastic zone of surrounding rock of noncircular roadways can be replaced by a virtual circle of equal area with "equivalent radius" as the characteristic size. The "equivalent radius" formula is

$$a = K\sqrt{\frac{S}{\pi}}. \tag{2}$$

In the above formula, $P_1$ is the original rock stress in the vertical direction of the roadway; $P_3$ is the original rock stress in the horizontal direction, and the supporting strength at the empty surface of the roadway is $P_i$; $c$ is the cohesion; $\varphi$ is the internal friction angle; $\lambda$ is the lateral pressure coefficient, that is, $P_3 = \lambda P_1$; $r$, $\theta$ are the polar coordinates of any point on the boundary of the plastic zone of the surrounding rock of the roadway; $S$ is the actual roadway section area; and $K$ is the roadway shape correction coefficient, reflecting the shape effect of the underground roadway; $K$ uses the parameters in Table 3.

Input the parameters measured on-site into MATLAB software, calculate the output to get Figure 9, and find out by analyzing Figure 9 and the calculation results, and the maximum depth of the plastic zone in the surrounding rock of the 3rd track uphill roadway is 7.4 m, which exceeds the length of the bolts and cables in the original support plan. That is to say, the anchoring sections of the bolt and the anchor cable are all within the plastic zone of the surrounding rock of the roadway, and the anchoring capacity is not fully utilized, which leads to large deformation of the roadway surrounding rock and failure anchoring. Therefore, in the design of roadway support, the length of the anchor cable must be greater than 7.4 m to ensure that the anchoring section of the anchor cable is in the complete rock body to avoid the occurrence of anchor failure problems.

*4.3. Roadway Surrounding Rock Support Plan.* Based on the analysis of the deformation characteristics of the surrounding rock of the track uphill roadway and the large-scale similar simulation test, combined with the actual situation of the site engineering, expand the construction of this roadway section. After reaching the original design size, the step-by-step combined support technology of "anchor mesh spray + full-face hollow grouting anchor cable" is adopted; namely, use metal nets, bolts, and shotcretes in the initial support. Full-face hollow grouting anchor cables are used for the second reinforced support. The specific support parameters and construction technology are as follows:

(1) For the initial support, the left-handed threaded steel bolts with a specification of Φ22 mm × $L$2800 mm are equipped with two 2535 resin coils, the distance between rows is 700 mm × 700 mm, and the anchor rods are connected by ladder beams; the metal mesh

Table 3: Correction coefficient of section shape of underground roadway.

| Section shape | Coefficient |
|---|---|
| Ellipse | 1.05 |
| Arch | 1.10 |
| Square | 1.15 |
| Positive trapezoid | 1.20 |
| Rectangle | 1.20 |
| Unilateral ladder | 1.25 |

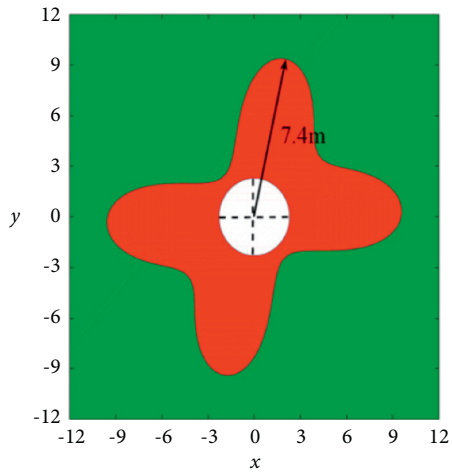


Figure 9: The distribution of plastic zone in roadway section.

uses 12 # iron wire diamond-shaped net; the grid is not larger than 40 mm. Spray 100 mm thick concrete to cover the metal mesh, as shown in Figure 10.

(2) The secondary reinforced support adopts full-face hollow grouting anchor cable, the specification of the anchor cable is $\Phi 22\,\text{mm} \times L12000\,\text{mm}$, the row distance between the anchor cables is $1500\,\text{mm} \times 1400\,\text{mm}$, and each anchor cable is equipped with 4 pieces of 2535 resin cartridges. The installation method is exactly the same as the ordinary resin anchor cable. The full-face hollow grouting anchor cable construction is carried out 30–40 m behind the heading face, and the grouting pressure is maintained at 8–10 MPa, as shown in Figure 11.

*4.4. Support Effect.* In order to verify the effect of "anchor network spraying + full-section hollow grouted anchor cable," the deformation of the surrounding rock was monitored. After the implementation of the support program, the top and bottom plates of the roadway and the two gangs were effectively controlled, and the deformation of the top and bottom plates was controlled within 217 mm, and the deformation of the two gangs was controlled within 301 mm, as shown in Figure 12. During the service period, no breakage of anchor cable and anchor rods was found, and no geological disaster such as roof and piece of the roadway surrounding rocks were found, which shows that the broken surrounding rocks form a good integrity under the action of slurry, which makes the anchor rods and

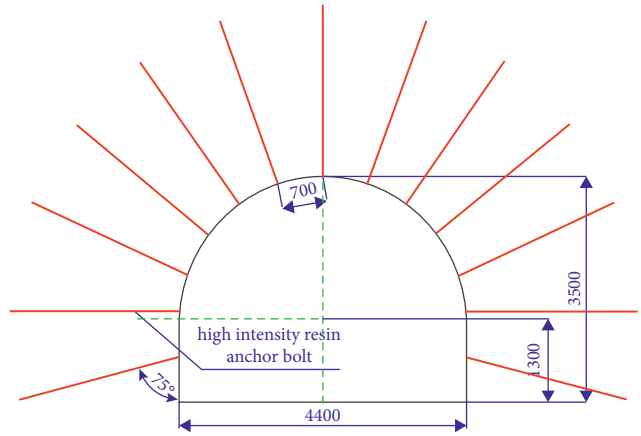


Figure 10: Cable "bolt + net" support.

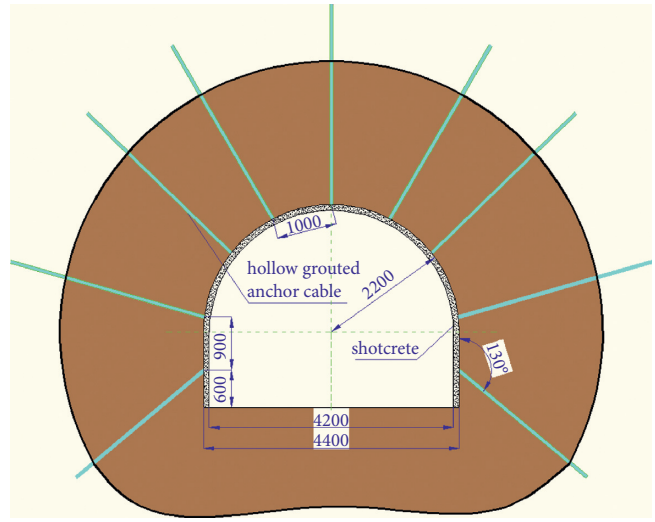


Figure 11: "Hollow grouting anchor cable + spray" support.

hollow grouting anchor ropes arranged in the roadway play a good role and have a better control effect, and can meet the safety production requirements.

## 5. Discussion

Through the above calculation results of the plastic zone and combined with the actual working conditions of the site, the control ideas under different support methods can be summarized in the following points: ① No matter what kind of support method is adopted, the fundamental purpose of its support is to strengthen the strength of the surrounding rock and improve the stability of the surrounding rock by controlling the expansion of the plastic zone. ② The "anchor mesh shotcrete + full-face hollow grouting anchor cable" combined support scheme proposed in this paper can be divided into two stages of support. Among them, the "anchor mesh shotcrete" is used in the first stage of support. The main purpose is to simply support the surrounding rock by anchoring and shotcreting and to provide certain help for the initial conditions of the second stage of support. The

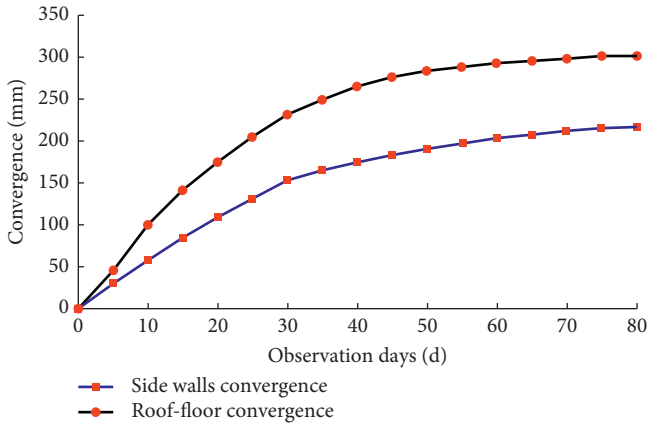


Figure 12: Convergence of roadway after support.

"full-face hollow grouting anchor cable" used in the second stage of support, and its main purpose is to "strengthen the roof and solidify" to carry out full-section strengthened support for the surrounding rock. ③ The biggest advantage of using hollow grouting anchor cable for grouting support is that the anchor cable is longer than the bolt, and it is easier to penetrate deeper rock formations. During grouting, the grout can be injected into the deep rock formations, so that the broken rock formations can be "connected" with the relatively stable deep rock formations, thereby controlling the expansion of the plastic zone and strengthening the stability of the surrounding rock.

## 6. Conclusions

(1) Mechanical tests were carried out on 25 sets of specimens with different proportions designed by the orthogonal method, and the best proportion of similar simulated materials for simulating the deformation and failure of the surrounding rock of the roadway was obtained.

(2) Using the large deep mine roadway simulation test system, a full-section excavation and unloading test of straight-wall arch roadway was carried out to realize the practical effect of roadway deformation and damage simulation under the path of "high stress + internal unloading + stress adjustment."

(3) After the deep roadway is excavated with preloaded high stress, the deformation and destabilization of the roadway surrounding rock mainly go through three periods: the first period is the period of uniform deformation of the roadway surrounding rock, the second period is the period of development of the roadway surrounding rock slab crack structure, and the third period is the period of destabilization of the roadway surrounding rock slab crack structure.

(4) Combined with the actual situation of the site project, the core of the hollow grouting anchor cable "anchor net spray + full-section hollow grouting anchor cable" step-by-step joint roadway repair support program was determined, and the stability of the repaired roadway was significantly improved to ensure the long-term use of the roadway.

## Data Availability

All the data generated or published during the study are included within the article; no other data were used to support this study.

## Conflicts of Interest

The authors declare that there are no conflicts of interest regarding the publication of this study.

## Acknowledgments

This work was financially supported by the Open Project of State Key Laboratory of Coking Coal Exploitation and Comprehensive Utilization, China Pingmei Shenma Group (Grant no. 41040220181107), the National Natural Science Foundation of China (1804109, 52074115, and 51874130), and the Natural Science Foundation of Hunan Province (2021JJ40211). The authors are grateful for this financial support.

## References

[1] Q. Wang, Q. Qin, B. Jiang, H. C. Yu, R. Pan, and S. C. Li, "Study and engineering application on the bolt-grouting reinforcement effect in underground engineering with fractured surrounding rock," *Tunnelling and Underground Space Technology*, vol. 84, pp. 237–247, 2019.

[2] T. Yang, J. Li, L. W. Wan, and S. Wang, "A simulation study on the spatial-temporal characteristics of pore water pressure and roof water inrush in an aquiclude," *Shock and Vibration*, vol. 2021, Article ID 6643894, 8 pages, 2021.

[3] C. Yuan, L. Fan, J. F. Cui, and W. J. Wang, "Numerical simulation of the supporting effect of anchor rods on layered and nonlayered roof rocks," *Advances in Civil Engineering*, vol. 2020, Article ID 4841658, 14 pages, 2020.

[4] C. Yuan, Y. N. Guo, W. J. Wang, L. M. Cao, L. Fan, and C. Huang, "Study on "triaxial loading-unloading-uniaxial loading" and microscopic damage test of sandstone," *Frontiers of Earth Science*, vol. 8, p. 11, 2020.

[5] F. Gao and H. Kang, "Experimental study on the residual strength of coal under low confinement," *Rock Mechanics and Rock Engineering*, vol. 50, no. 2, pp. 285–296, 2017.

[6] C. Yuan, L. M. Cao, L. Fan, and J. Q. Guo, "Theoretical analysis on distribution pattern of plastic zone in surrounding rock of high-gas-coal roadway," *Advances in Civil Engineering*, vol. 2021, Article ID 6684243, 17 pages, 2021.

[7] L. Tang and S. Liang, "Study on the feasibility of the upward mining above the goaf of the irregular roadway mining under the influence of hard and thick strata," *Geotechnical & Geological Engineering*, vol. 37, no. 6, pp. 5035–5043, 2019.

[8] Z. L. Xu, Y. B. Luo, J. X. Chen, Z. M. Su, T. T. Zhu, and J. P. Yuan, "Mechanical properties and reasonable proportioning of similar materials in physical model test of tunnel lining cracking," *Construction and Building Materials*, vol. 300, Article ID 123960, 13 pages, 2021.

[9] H. Zhou, J. J. Lu, S. C. Hu, C. Q. Zhang, R. C. Xu, and F. Z. Meng, "Influence of curvature radius of tunnels excavation section on slabbing of hard brittle rockmass under high

stress," *Rock and Soil Mechanics*, vol. 37, no. 1, pp. 140–146, 2016.

[10] C. Y. Liu, G. M. Zhao, W. S. Xu, and X. R. Meng, "Experimental study on rockburst and its spatio-temporal evolu-tion criterion in high stress roadway," *Journal of China Coal Society*, vol. 45, no. 3, pp. 998–1008, 2020.

[11] H. W. Jing, Q. Yin, D. Zhu, Y. J. Sun, and B. Wang, "Experimental study on the whole process of instability and failure of an-chorage structure in surrounding rock of deep-buried roadway," *Journal of China Coal Society*, vol. 45, no. 3, pp. 889–901, 2020.

[12] J. Li, W. Wang, B. Li, J. Tan, and B. Peng, "Directionality of butterfly leaves and nonuniform deformation mechanism in gob-side entry driving roadway," *Journal of Mechanics*, vol. 37, no. 11, pp. 291–301, 2021.

[13] H. P. Kang, P. F. Jiang, J. W. Yang et al., "Roadway soft coal control technology by means of grouting bolts with high pressure-shotcreting in synergy in more than 1 000 m deep coal mines," *Journal of China Coal Society*, vol. 46, no. 3, pp. 747–762, 2021.

[14] S. R. Xie, G. Q. Xie, S. S. He et al., "Anchor-spray-injection strengthened bearing arch supporting mechanism of deep soft rock roadway and its application," *Journal of China Coal Society*, vol. 39, no. 3, pp. 404–409, 2014.

[15] Y. L. Yang, X. B. Li, and P. F. Li, "Study on surrounding rock deformation mechanism and control of roadway with large section and extra-thick top coal," *Shock and Vibration*, vol. 2021, Article ID 6618424, 11 pages, 2021.

[16] G. Y. Yu, J. Wang, J. J. Ren et al., "Study on surrounding rock structure evolution characteristics and roof control techniques of the retained roadway formed by roof cutting in inclined coal seams," *Shock and Vibration*, vol. 2021, Article ID 7491887, 20 pages, 2021.

[17] X. Y. Xiong, J. Dai, and X. N. Chen, "Analysis of stress asymmetric distribution law of surrounding rock of roadway in inclined coal seam: a case study of shitanjing No. 2 coal seam," *Advances in Civil Engineering*, vol. 2020, Article ID 8877172, 14 pages, 2020.

[18] J. Liu and G. Y. Jiang, "Use of laboratory indentation tests to study the surface crack propagation caused by various indenters," *Engineering Fracture Mechanics*, vol. 241, p. 11, Article ID 107421, 2021.

[19] J. Liu, J. Wang, and W. Wan, "Numerical study of crack propagation in an indented rock specimen," *Computers and Geotechnics*, vol. 96, pp. 1–11, 2018.

[20] J. Li, X. B. Qiang, W. S. Wang, and F. Wang, "Distribution law of principal stress difference of deep surrounding rock of gob-side entry and optimum design of coal pillar width," *Tehnički Vjesnik*, vol. 26, no. 6, pp. 1743–1752, 2019.

[21] J. Li, "The coal pillar design method for a deep mining roadway based on the shape of the plastic zone in surrounding rocks," *Arabian Journal of Geosciences*, vol. 2020, p. 12, 2020.

[22] J. Lin, Y. Wang, J. H. Yang, Z. S. Wang, and J. F. Cai, "Simulation studies on stress field evolution of roadway excavation under different confining pressures," *Journal of China Coal Society*, vol. 40, no. 10, pp. 2313–2319, 2015.

[23] F. Q. Gong, Y. Luo, X. F. Si, and X. B. Li, "Experimental modelling on rockburst in deep hard rock circular tunnels," *Chinese Journal of Rock Mechanics and Engineering*, vol. 36, no. 7, pp. 1634–1648, 2017.

[24] C. Yuan, L. Cao, W. Wang, L. Fan, and C. Huang, "Case study on rock support technology for roadways based on characteristics of plastic area," *KSCE Journal of Civil Engineering*, vol. 25, no. 2, pp. 705–723, 2021.